Liquid-liquid phase separation of florigen activation complex induces flowering

Ken-ichiro Taoka[1†*], Hiroyuki Tsuji[1†*], Suai Anzawa[2], Mayu Enomoto[2], Yuka Koizumi[2], Juri Nakamura[1], Mari Tanaka[1], Akiko Fujita[3], Kyoko Furuita[4], Takashi S. Kodama[4], Masaru Fujimoto[5], Kazuo Kurokawa[6], Takashi Okamoto[7], Toshimichi Fujiwara[4], Akihiko Nakano[6], Chojiro Kojima[2, 4*]

[1]Kihara Institute for Biological Research, Yokohama City University, Yokohama, Japan

[2]Graduate School of Engineering Science, Yokohama National University, Yokohama, Japan

[3]Graduate School of Biological Sciences, Nara Institute of Science and Technology, Nara, Japan

[4]Institute for Protein Research, Osaka University, Suita, Osaka, Japan

[5]Graduate School of Agricultural and Life Sciences, The University of Tokyo, Tokyo, Japan

[6]Live Cell Super-Resolution Imaging Research Team, RIKEN Center for Advanced Photonics, Wako, Saitama, Japan

[7]Department of Biological Sciences, Tokyo Metropolitan University, Minami-osawa, Hachioji, Tokyo, Japan

[†]These authors contributed equally to this work.

*Corresponding authors: ktaoka@yokohama-cu.ac.jp, tsujih@yokohama-cu.ac.jp, kojima-chojiro-xk@ynu.ac.jp

Abstract

Floral transition, regulated by the systemic action of the mobile florigen protein FLOWERING LOCUS T (FT), is essential for successful plant reproduction[1]. How FT controls downstream gene expression remains incompletely understood, although it relies on the florigen activation complex (FAC), a core component of FT function[2–4]. The FAC is a nucleus-localized transcriptional activator of genes encoding MADS-box transcription factors critical to reproductive development and consists of florigen FT; a scaffold 14-3-3 protein that is a key component for complex assembly; and FD, a basic leucine-zipper protein that recruits the FAC to DNA. Here we report that the FAC exhibits phase separation. In rice shoot apical meristem cells, rice florigen Heading date 3a (Hd3a) fused to the green fluorescent protein formed speckles in the nucleus. The FAC speckle is formed in a FAC-dependent manner in tobacco cells. Recombinant Hd3a, but not OsFD1, phase-separated in vitro, and this effect was enhanced in the presence of 14-3-3 protein. Furthermore, mutations affecting functionally important residues in the pocket region or C-terminal disordered region of Hd3a affected FAC phase separation, providing a biochemical framework for the protein's effect on flowering. The ability to form condensates via phase transition represents a previously unknown mechanism for gene activation by the FAC.

Main

Florigen is a systemic signal that induces flowering[5,6] whose molecular identity was elucidated with the cloning of Arabidopsis (*Arabidopsis thaliana*) *FLOWERING LOCUS T* (*FT*) and orthologues from other plant species, such as *HEADING DATE 3A* (*Hd3a*) in rice (*Oryza sativa*)[1,7,8]. *FT*, *Hd3a* and orthologues are expressed and translated in leaves and then transported to the shoot apical meristem (SAM) responsible for the production of all above-ground tissue[7,9,10]. Next, the SAM is converted from a leaf-forming vegetative meristem to a

50 flower-forming reproductive meristem through the formation of the florigen activation
51 complex (FAC), comprising the florigen itself, the florigen receptor 14-3-3 protein and the
52 basic leucine zipper (bZIP) transcription factor FD[2–4,11,12]. Although great strides have been
53 made in understanding florigen function, the biochemical mechanisms by which the FAC
54 activates downstream gene expression are not well understood. As a first step toward
55 elucidating these, we determined the subcellular localization of the FAC. We performed super-
56 resolution imaging microscopy by stimulated emission depletion (STED)[13,14] of cells in the
57 rice SAM. Because Hd3a is expressed in the phloem of vascular bundles[7,15,16], we generated
58 rice plants expressing *green fluorescent protein* (*GFP*) or *Hd3a-GFP* driven by the *rolC*
59 promoter from *Agrobacterium rhizogenes*, which is highly active in the phloem [7,17,18]. The
60 resulting translated GFP and Hd3a-GFP were transported to the SAM, where they accumulated
61 in cell nuclei (Fig. 1a,b). As a control for STED, we determined the localization of histone H2B
62 fused to GFP (H2B-GFP)[19] in the nucleus of SAM cells, revealing punctate signals and
63 exclusion from the nucleolus indicative of the nucleosome (Fig. 1c). Free GFP showed a faint
64 signal in the cytoplasm and was uniformly distributed in the nucleus, whereas Hd3a-GFP
65 formed speckle-like structures in the nucleus (Fig. 1d,e). To confirm the formation of Hd3a-
66 containing speckles, we visualized GFP fluorescence from the nuclei of SAM cells of
67 transgenic plants harbouring the *Hd3apro:Hd3a-GFP* transgene[7] by super-resolution confocal
68 live imaging microscopy (SCLIM)[20,21], a super-resolution imaging technique based on
69 principles distinct from those underlying STED. However, as observed by STED, Hd3a-GFP
70 defined a speckle-like structure in the nuclei of rice SAM cells (Fig. 1f,g,h).
71
72 Cellular speckle-like structures have recently been proposed to constitute biomolecular
73 condensates, i.e., phase separation[22–27]. To assess whether the observed speckle-like Hd3a
74 structures are caused by liquid condensates, we purified recombinant Hd3a and its paralogue

rice FT1 (RFT1) and examined their ability to form condensates in vitro. Indeed, both recombinant Hd3a and RFT1 proteins appeared to form condensates, with a diameter of about 10 µm, in vitro in solutions containing polyethylene glycol (PEG) (Fig. 1i,j). To characterize these condensates, we measured their absorbance in the range of 330–800 nm, as absorbance over this range indicates the degree of condensation and reflects the size of the dispersed condensates in solution: larger condensates show a constant absorbance, as illustrated with glass beads of different diameters in solution (Extended Data Fig. 1). Hd3a showed a constant absorbance over the measurement range (Fig. 1k) that was reminiscent of the pattern seen for large-size glass beads, suggesting the presence of large condensates containing Hd3a and RFT1 (Extended Data Fig. 2). This result was consistent with microscopic observations of the larger condensates with roughly 10-µm condensates. Furthermore, recombinant Hd3a and RFT1 formed spherical condensates rather than aggregated precipitates (Fig. 1i,j), indicating that Hd3a and RFT1 undergo liquid phase separation in vitro.

Transient expression of *Hd3a* and *OsFD1* in rice protoplasts reconstituted the FAC by complexing with endogenous 14-3-3 proteins, leading to the activation of one of its transcriptional targets, *OsMADS15*, which encodes a MADS-box transcription factor[2,28] (Fig. 2a). FAC reconstitution has also been reported from the transient expression of Arabidopsis *FT* and *FD* or rice *FD4* and *RFT1* in *N. benthamiana* leaves[11,29]. To investigate whether nuclear speckles form upon reconstitution of the FAC, we transiently expressed *Hd3a-GFP* and *OsFD1* in *N. benthamiana* leaves and determined the green fluorescence pattern detectable in their nuclei. The mean number of speckles per nucleus was small (less than 0.5) when *Hd3a* alone or *OsFD1* alone was expressed, while nuclei contained an average of three speckles upon co-expression of *Hd3a* and *OsFD1* (Fig. 2b,c). This observation suggests that FAC formation entails the localization of Hd3a into nuclear speckles.

100

101 To characterize whether these nuclear speckles formation is explained by condensate formation
102 in vitro, we measured the absorbance of recombinant Hd3a, 14-3-3 protein GF14c[2] and OsFD1
103 alone or in mixtures over the range of 330–800 nm. We were unable to prepare a large amount
104 of full-length OsFD1, but we succeeded in preparing a C-terminal truncated version of OsFD1
105 that retains the coiled-coil region. Hd3a showed constant absorbance over the measurement
106 range, whereas 14-3-3 and OsFD1 showed little absorbance on their own (Fig. 2d,e). To
107 determine the effect of 14-3-3 protein on condensate formation by Hd3a or OsFD1, we added
108 14-3-3 protein to recombinant Hd3a or OsFD1 and measured the absorbance of the resulting
109 mixtures. The absorbance was higher when 14-3-3 was included than with recombinant Hd3a
110 or OsFD1 protein alone (Fig. 2d,e). We next added recombinant 14-3-3 protein to a mixture of
111 recombinant Hd3a and OsFD1 proteins and measured the absorbance of the resulting solution
112 (Fig. 2e), finding that the mixture displayed a constant absorbance of about 0.2. The absorbance
113 increased considerably when recombinant 14-3-3 protein was added to the mixture (Fig. 2e).
114 Increasing ratio of Hd3a against 14-3-3 resulted in higher absorbance (Extended Data Fig.3).
115 These results suggest that the formation of the three-protein FAC promotes the appearance of
116 condensates in vitro.

117

118 To better understand FAC function, we examined whether the interaction between Hd3a and
119 14-3-3 is required to form nuclear speckles. Accordingly, we introduced mutations in Hd3a
120 that abolish its interaction with 14-3-3 proteins. The phenylalanine 103 (F103), arginine 64
121 (R64) and arginine 132 (R132) residues of Hd3a form a hydrogen bond that is essential for
122 interaction with 14-3-3 proteins, and their mutation to create $Hd3a^{F103A}$ or $Hd3a^{R64K,R132K}$
123 mutants abolished the interaction between Hd3a and 14-3-3 interaction and resulted in a loss
124 of FAC transcriptional activity[2] (Fig. 2a). Neither *Hd3a*^{F103A}*-GFP* nor *Hd3a*^{R64K,R132K}*-GFP* led

125 to the formation of nuclear speckles when transiently expressed in *N. benthamiana* leaves (Fig.
126 2c, 3a). To investigate whether the interaction between Hd3a and 14-3-3 is necessary for
127 condensate formation, we performed an in vitro assay in which we added recombinant 14-3-3
128 protein to mutant recombinant Hd3a and measured the absorbance of the solutions. The
129 absorbance of recombinant $Hd3a^{F103A}$ and $Hd3a^{R64K,R132K}$ in the presence of recombinant 14-
130 3-3 protein was lower than that of intact Hd3a with 14-3-3 (Fig. 3b,c). These results indicate
131 that the interaction between Hd3a and 14-3-3 is a prerequisite for condensate formation.
132
133 The family of phosphatidylethanolamine-binding proteins (PEBP), to which florigen belongs,
134 is characterized by an anion-binding pocket that has been suggested to play an important role
135 in the function of florigen[30,31]. The tyrosine 87 (Y87) residue is located deep in this potential
136 ligand-binding pocket on the surface of florigen and is conserved across all FT orthologues,
137 but is replaced by histidine in TERMINAL FLOWER 1 (TFL1) and its orthologues, floral
138 repressors that are closely related to FT[32]. To explore the potential link between the pocket and
139 condensate formation, we characterized a mutant version of Hd3a harbouring histidine instead
140 of tyrosine at residue 87 (Y87H). $Hd3a^{Y87H}$ failed to activate *OsMADS15* expression (Fig. 2a)
141 but retained the ability to form nuclear speckles (Fig. 4a,b) and condensates in vitro (Fig. 4c).
142 These results indicate that the Y87H mutation in the pocket region causes loss of transcriptional
143 activation by the FAC without affecting nuclear condensate formation.
144
145 We also examined the link between FAC function and condensate formation for other known
146 loss-of-function mutations, namely those corresponding to the Arabidopsis *ft-1* and *ft-3* alleles.
147 The FT protein in the *ft-1* mutant contains two consecutive glycine residues (G) in the C-
148 terminal disordered region, one of which is mutated to glutamic acid (E)[15,16,33,34]. A transient
149 expression assay revealed that the equivalent mutant in rice Hd3a is G173E, as it failed to

activate *OsMADS15* transcription (Fig. 2a). We next examined whether Hd3a^{G173E} can form nuclear speckles. We discovered that *Hd3a*^{G173E} could not form nuclear speckles when transiently expressed in *N. benthamiana* leaf cells (Fig. 4a,b). Likewise, recombinant Hd3a^{G173E} suppressed condensate formation when incubated with recombinant 14-3-3 protein in vitro (Fig. 4d). Since the G173 residue is located in the C-terminal disordered region of Hd3a[2,34], this substitution does not affect the overall structure. Thus, the behaviour of the Hd3a^{G173E} mutant underscores the importance of the C-terminal disordered region following FAC formation.

The Arabidopsis *ft-3* allele is equivalent to a mutant of Hd3a in which arginine 121 is replaced by histidine (R121H)[15,16,33]. The R121 residue is located internally within the Hd3a structure. Hd3a^{R121H} can interact with 14-3-3 proteins[2] but appeared to have partially lost its transcriptional activation potential (Fig. 2a). When we transiently expressed Hd3a^{R121H} in *N. benthamiana* leaf cells, we observed that it could not form nuclear speckles (Fig. 4a), and it inhibited condensate formation in the presence of 14-3-3 protein to a greater extent than intact Hd3a in vitro (Fig. 4e). Since R121 is embedded in the Hd3a molecule[2,34], we investigated whether R121H disrupted the structure of Hd3a. Indeed, the structure of Hd3a^{R121H} appeared to be different from WT, since the nuclear magnetic resonance (NMR) spectrum of Hd3a^{R121H} was different from WT (Extended Data Fig. 4). These results suggest that R121H is a mutation that prevents condensate formation by changing the protein structure of Hd3a while maintaining its interaction surface with 14-3-3 proteins.

Collectively, our results suggest that the FAC exerts its transcriptional activation through a mechanism that involves nuclear speckles and condensation and that depends on the conserved R121 residue and the C-terminal disordered region of Hd3a (to which the G173 residue maps).

Although the mechanism of condensate formation by florigen is currently unknown, we hypothesize that it involves a multivalent interaction such as charge interactions between FAC components. For example, the surface of florigen is basic, while that of 14-3-3 is acidic[2,35]. The electrostatic interactions based on these differences may induce a multivalent interaction between florigen and 14-3-3 to promote condensate formation. In addition, the phosphorylated SAP motif of FD may help bridge multiple 14-3-3 dimers to facilitate condensate formation through multivalent interactions.

The results of this study suggest that condensate formation serves as a mechanism by which the FAC activates downstream gene expression (Fig. 4f). Interaction between Hd3a and FD mediated by 14-3-3 protein is essential for condensate formation, and the Hd3a C-terminal disordered region containing the G173 residue promotes this process after FAC assembly. This multi-layered regulation along with condensate formation contributes to FAC-mediated transcriptional activation.

Phase-separated condensation of FAC may provide a cooperative switching mechanism for gene expression related to flowering. The phase-separated condensation of FAC occurs when all required proteins are simultaneously present in high concentrations in a cell: for FAC, Hd3a, 14-3-3 and OsFD1. In rice SAMs, 14-3-3 and OsFD1 accumulate in high concentrations in the cells during the vegetative phase[36]. Therefore, the phase-separated condensation of FAC may provide a cooperative switching mechanism whereby Hd3a is transported into the SAM and its concentration is increased, and the phase-separated condensation of FAC and transcriptional activation occur only when the concentrations of Hd3a, 14-3-3 and OsFD1 are sufficiently high.

200

201 **Methods**

202 ***Plant materials and growth conditions***

203 Rice (*Oryza sativa* L. subspecies *japonica*) variety Nipponbare was used as wild type.
204 *Hd3apro*:*Hd3a–GFP*, *rolCpro*:*Hd3a–GFP, rolCpro*:*GFP* and *Ubqpro*:*H2B–GFP* transgenic
205 rice plants were described previously[7,19]. Transgenic rice cell lines derived from the
206 *OsMADS15-nanoLuc* gene targeting line (*M15NL-KI*) were described previously[28]. Transgenic
207 rice plants were generated using Agrobacterium (*Agrobacterium tumefaciens*)-mediated
208 transformation of rice calli, as previously described, and hygromycin-resistant plants were
209 regenerated from the transformed calli[7]. Plants were grown in growth chambers at 70%
210 humidity, under short-day conditions with daily cycles of 10 h of light at 28 °C and 14 h of
211 darkness at 25 °C. Light was provided by white fluorescent tubes (400–700 nm, 100 μmol m^{-}
212 ^{2} s^{-1}). Cells from rice suspension cultures were maintained as described previously. *Nicotiana*
213 *benthamiana* plants were grown under long-day conditions with daily cycles of 16 h of light at
214 22 °C and 8 h of darkness at 20 °C. Light was provided by white fluorescent tubes (400–
215 700 nm, 100 μmol m^{-2} s^{-1}).

216

217 ***Plasmid construction***

218 To make an expression vector in rice protoplast, a 2005-bp fragment of maize ubiquitin
219 promoter and a 252-bp fragment of NOS terminator were amplified by PCR. A 1784-bp of
220 Gateway recombination site were obtained by digestion of pGWB26 vector[36] with restriction
221 enzymes, XbaI and SacI. These three fragments were inserted into pGreen II plasmid[37] to
222 make the expression vector, pGIIpUbqGWT7Ct. Mutations in Hd3a were introduced by PCR
223 mutagenesis with a designed primer set. The resultant Hd3a mutants were cloned into

224 pENTR-D-TOPO (Thermo Fisher Scientific) and introduced into pGIIpUbqGWT7Ct with
225 LR clonase II (Thermo Fisher Scientific). For OsFD1 expression, pUbq-OsFD1[2] was used.
226 For Agroinfiltration in tobacco, pGWB602 or pGWB605[38] were used for the destination
227 vectors.
228
229 ***Agroinfiltration***
230 Agroinfiltration was performed as described previously[39]. The Agrobacterium strains EHA105
231 and MP90 were used for transformation of pGWB602 or pGWB605 derivatives[38] and pBIC
232 p19[40], respectively. pBIC p19 harbours the silencing suppressor p19 from tomato bushy stunt
233 virus (TBSV). After overnight growth in LB medium, agrobacteria were collected by
234 centrifugation and resuspended to an OD_{600} = ~0.6 in infiltration buffer (2 mg ml^{-1}
235 $MgCl_2 \cdot 6H_2O$, 150 μM acetosyringone, 10 mg ml^{-1} MES-KOH, pH 5.6). The appropriate
236 combinations of cell suspensions were mixed in equal volumes and infiltrated into *N.*
237 *benthamiana* leaves 4–5 weeks after germination with a 1-mL syringe. The cells were fixed
238 with 4 % paraformaldehyde for 5-6 days after infiltration and observed within a month.
239
240 ***Imaging by confocal laser scanning microscopy***
241 The shoot apical meristems (SAMs) from transgenic rice plants were dissected under a
242 microscope[41]. For imaging by stimulated emission depletion (STED), SAMs were fixed by 4%
243 paraformaldehyde and cleared with ClearSee, stained by SCRI SR2200 for cell wall staining
244 and visualized using a confocal laser-scanning microscope (TCS SP8; Leica Microsystems,
245 Tokyo, Japan) equipped with 592-nm STED laser, a 405-nm laser and a pulsed white-light
246 laser (WLL) line and 93· oil-immersion objective lens. Samples were excited with the 488-nm
247 wavelength of the WLL (80 MHz) and depleted with the 592-nm STED laser. Collected images
248 were deconvolved using the default settings of the STED module in Huygens Professional

249 Deconvolution software. For imaging by super-resolution confocal live imaging microscopy
250 (SCLIM), SAMs were dissected and visualized without fixation. GFP was excited with the
251 473-nm laser. The fluorescence emission spectra were separated with the custom-made
252 dichroic mirror and filtered through a 490-545 bandpass filter. Images were acquired with an
253 ImagEM EM-CCD camera (Hamamatsu Photonics). High-resolution images were constructed
254 via deconvolution analysis performed with Volocity (PerkinElmer). A three-dimensional
255 SCLIM image was constructed from 40 images taken at 0.1-μm vertical intervals using a
256 theoretical point-spread function optimized for CSU10 confocal microscopes (Yokogawa
257 Electric). *N. benthamiana* epidermal leaf cells were visualized with a confocal laser-scanning
258 microscope (LSM 880; Zeiss, Tokyo, Japan) equipped with a 488-nm source and a 63×
259 glycerol-immersion objective lens. For GFP fluorescence, images were captured at 500–
260 600 nm after excitation at 488 nm. After image acquisition, the images were processed using
261 Zen software (Zeiss).
262
263 ***Recombinant protein production and purification***
264 The coding sequence of *Hd3a* and RFT1 were cloned into the pCold-GST vector[42] and
265 produced as a glutathione S-transferase (GST) fusion protein in *Escherichia coli* BL21 Rosetta
266 (DE3) (Novagen). Cells were grown in LB medium or minimal medium containing 0.5 g l^{-1}
267 of ^{15}N-ammonium chloride. Recombinant GST fusion protein was purified with glutathione
268 Sepharose 4B resin (Cytiva). After removal of the GST tag using GST-HRV 3C protease, Hd3a
269 was purified by gel filtration chromatography using a Superdex75 column (Cytiva) with 50
270 mM potassium phosphate buffer (pH 6.8) containing 50 mM KCl and 1 mM dithiothreitol
271 (DTT). To prepare Hd3a point mutants, plasmids were constructed by PCR using KOD plus
272 DNA polymerase (TOYOBO) and the resulting recombinant proteins were purified essentially
273 as described above.

274 The coding sequence of the 14-3-3 gene *GF14c*[43] was cloned into the pCold-GST vector.
275 GF14c was produced as a GST fusion protein in *E. coli* BL21 Rosetta (DE3) and purified with
276 Glutathione Sepharose 4B resin and a Superdex 200 column (Cytiva), followed by removal of
277 the GST tag.
278 The coding sequence of *OsFD1*[2] was cloned into the pCold-GST vector. We could not purify
279 the large amount of recombinant full-length protein. We therefore turned to a N-terminal-
280 truncated version of OsFD1 (147–195) (lacking amino acids 1–146) with the S192E mutation,
281 which was produced as a GST fusion protein in *E. coli* BL21 Rosetta (DE3) and purified as
282 above.

283 ***In vitro protein phase separation***

284 Polyethylene glycol 8,000 (BioUltra grade, Sigma-Aldrich) was added to protein samples to a
285 final concentration of 15% (w/v) in 25 mM potassium phosphate buffer (pH 6.8) containing
286 25 mM KCl and 0.5 mM DTT. The solutions were incubated for 24 h at 4 °C for protein phase
287 separation. Phase separation was then assessed by measuring protein solution turbidity from
288 200 µl of protein solution (absorbance scanned between 330 and 800 nm) in 96-well plates
289 (Stem, Tokyo) with a spectral scanning multimode reader (VarioSkan Flash 2.4, Thermo
290 Fisher). Total protein concentration was 100 µM for all samples except for R121H mutant
291 where 50 µM was used due to the difficulty in concentrating the protein solution. For phase-
292 contrast image analyses, a Leica DMI300B microscope was used. The droplets of condensed
293 Hd3a and RFT1 proteins were spherical and were hard to merge with each other even over a
294 long lifetime, much like aging Maxwell glass.[44].
295

296 ***Nuclear magnetic resonance (NMR) experiments***

297 All NMR spectra were acquired on an AVANCE III HD 800 spectrometer (Bruker) at 303 K,
298 processed and analysed with TopSpin 4.11 software. ^{1}H-^{15}N HSQC experiments on 0.057 mM

299 ^{15}N-labelled Hd3a mutants were performed in 50 mM potassium phosphate buffer (pH 6.8)
300 containing 50 mM KCl and 1 mM DTT.
301
302 ***Protoplast transformation***
303 Transformation of rice protoplasts was performed as described previously[2,28]. Five micrograms
304 of *Hd3a* and *OsFD1* effector constructs and 0.5 µg of pUbqFluc reporter plasmid[2] were
305 transfected into 0.3–1.0 × 10^7 protoplasts per ml by the PEG-mediated transformation method.
306 After a 24-h incubation at 30 °C, the protoplast suspension was centrifuged and the cell pellet
307 was frozen at −80 °C for measurement of luciferase activity.
308
309 ***Measurement of luciferase activity in protoplast lysates***
310 Luciferase activity was measured as described previously[28]. The activities derived from
311 NanoLuc (Nluc) and firefly luciferase (Fluc) in the lysates were measured separately and their
312 ratio calculated. The Nano-Glo Luciferase Assay System (Promega) and Dual Luciferase
313 Reporter Assay System (Promega) were used according to the manufacturer's instructions for
314 Nluc and Fluc activity, respectively. Transfected protoplasts were lysed with 25 µl of Passive
315 lysis buffer (Promega). Nluc luminescence was measured with a TriStar LB941 microplate
316 reader (Berthold Technologies) immediately after mixing of 10 µl of lysate and 10 µl of Nano-
317 Glo Luciferase Assay Reagent in a 96-well plate. Fluc luminescence was measured
318 immediately after mixing 2 µl of lysate and 10 µl of LARII Reagent in a 96-well microtiter
319 plate.
320

321 ***Data availability***

322 The plasmids for transient expressions, plant transformations and protein purifications are
323 available upon requests. Any other relevant data are available from the corresponding authors upon
324 reasonable request.

325

326 **Figure legends**

327 **Fig. 1 | Hd3a forms nuclear speckles in the shoot apical meristem.**

328 **a**,**b**, Representative GFP fluorescence pattern from *GFP* (**a**) or *Hd3a-GFP* (**b**) constructs
329 driven by the phloem-specific *rolC* promoter in the rice shoot apical meristem. Scale bars, 10
330 μm. **c–e**, Stimulated emission depletion (STED) imaging of cells within the rice shoot apical
331 meristem harbouring the transgenes *Ubqpro:H2B-GFP* (**c**), *rolCpro:GFP* (**d**) and
332 *rolCpro:Hd3a-GFP* (**e**). **f**, Super-resolution confocal live imaging microscopy (SCLIM)
333 imaging of cells in the rice shoot apical meristem harbouring the transgene *Hd3apro:Hd3a-*
334 *GFP*. Scale bars, 5 μm. **g**, Enlarged view of the region highlighted by a dashed box in (**f**). **h**,
335 Enlarged view of a nucleus in the shoot apical meristem from a *Hd3apro:Hd3a-GFP* transgenic
336 rice line. **i**,**j**, Spherical condensates of Hd3a (**i**) and RFT1. Scale bars, 10 μm. (**j**). **k**, Absorbance
337 of recombinant Hd3a in a PEG-containing solution.

338

339 **Fig. 2 | Formation of the florigen activation complex (FAC) facilitates nuclear speckle**
340 **formation and in vitro condensation.**

341 **a**, Effects of Hd3a mutations on *OsMADS15* transcriptional activation. **b**, Hd3a-GFP
342 localization in the nucleus of *N. benthamiana* leaf epidermal cells. Scale bars, 10 μm. **c**, Effects
343 of Hd3a mutations on the mean number of nuclear speckles. **d**,**e**, Absorbance of recombinant
344 Hd3a alone (red), GF14c alone (blue) and Hd3a with GF14c (purple) (**d**) and of OsFD1 alone
345 (light green), Hd3a with OsFD1 (brown) and Hd3a with OsFD1 and GF14c (black) (**e**).

346

347 **Fig. 3 | Interaction with 14-3-3 protein facilitates nuclear speckle formation and in vitro**
348 **condensation of Hd3a.**

349 **a**, Localization pattern of Hd3a^{R64K,R132K}-GFP and Hd3a^{F103A}-GFP when co-expressed with
350 *OsFD1* in the nucleus of *N. benthamiana* leaf cells. Scale bars, 10 μm. **b**,**c**, Absorbance of
351 recombinant Hd3a with GF14c (green) and Hd3a^{R64K,R132K} with GF14c (black) (**b**) and of Hd3a
352 with GF14c (green) and Hd3a^{F103} with GF14c (black) (**c**). Scale bars, 10 μm.

353

354 **Fig. 4 | Substitutions in the potential ligand-binding pocket and C-terminal disordered**
355 **region of Hd3a modulate nuclear speckle formation and in vitro condensation.**

356 **a**, Localization pattern of Hd3a^{Y87H}-GFP, Hd3a^{R121H}-GFP and Hd3a^{G173E}-GFP when co-
357 expressed with *OsFD1* in the nucleus of *N. benthamiana* leaf cells. Scale bars, 10 μm. **b**,
358 Effects of Hd3a mutations on the number of nuclear speckles. **c**–**e**, Absorbance of recombinant
359 Hd3a with GF14c (green throughout) and of Hd3a^{Y87H} with GF14c (black, **c**), Hd3a^{R121H} with
360 GF14c (black, **d**) and Hd3a^{G173E} with GF14c (black, **e**), mixed 50:50 in each case. **f**, Proposed
361 model of FAC activity through condensate formation by condensate formation in the nucleus.
362 FAC formation induces condensate formation, which requires the interaction of Hd3a with 14-
363 3-3 via the Hd3a residues R64, F103 and R132. G173 in the C-terminal disordered region and
364 the internal R121 are essential for condensate formation after FAC formation. The potential
365 anion-binding pocket of Hd3a includes Y87, which is essential for FAC function but is
366 dispensable for condensate formation, suggesting that it acts downstream of condensate
367 formation.

368

369

Extended Data Fig. 1 | Changes in the absorbance of suspensions consisting of glass beads of different sizes.

Absorbance between 330 and 800 nm of glass bead solutions with diameters of 3 μm, 200 nm and 70 nm.

Extended Data Fig. 2 | Absorbance of RFT1 with or without the 14-3-3 protein GF14c.

Absorbance between 330 and 800 nm of recombinant RFT1 protein with (purple) or without (magenta) GF14c.

Extended Data Fig. 3 | Ratio dependence of absorbance in Hd3a and GF14c.

Absorbance between 330 and 800 nm of recombinant Hd3a with GF14c mixed in ratios of 50:50 (blue) or 25:75 (purple).

Extended Data Fig. 4 | NMR spectra of Hd3a WT and R121H.

^{1}H–^{15}N heteronuclear single quantum coherence (HSQC) spectra of ^{15}N-labelled recombinant Hd3a proteins for wild-type (WT, blue) and R121H mutant (red). p.p.m., parts per million.

Acknowledgements

We thank Momoko Yoneyama for her technical support and Prof. Kentaro Shiraki for his comments on in vitro phase-separation experiments. This study was supported in part by MEXT/JSPS KAKENHI, Grant-in-Aid for Scientific Research (C), number 17K07609 to K.T., Grants-in-Aid for Scientific Research on Innovative Areas (numbers 16H06464 and 16H06466 to H.T., and 17H05836 and 19H04856 to C.K.), Grant-in-Aid for Scientific Research (B)

(number 20H03191 to C.K.), Grant-in-Aid for Scientific Research (A) (number 16H02532 and 21H04728 to H.T.), a Core Research for Evolutionary Science and Technology (CREST) grant from the Japan Science and Technology Agency (JST) JPMJCR16O4 to H.T., Platform for Drug Discovery, Informatics, and Structural Life Science by MEXT, Platform Project for Supporting Drug Discovery and Life Science Research (Basis for Supporting Innovative Drug Discovery and Life Science Research, BINDS; number JP21am0101072) through the Japan Agency for Medical Research and Development, and the Collaborative Research Program of the Institute for Protein Research, Osaka University (CR-20-02).

Author contributions

K.T., H.T. and C.K. designed the research, interpreted data and wrote the manuscript with the inputs from all authors.. K.T. performed transient expression analysis. S.A., M.E., Y.K. performed phase-separation assays. K.F. performed NMR measurements. T.K. and T.F. supervised protein analysis. M.T. performed microscopic observations of transient assays and plant transformation. J.N., A.F., M.F. and K.K. performed super-resolution imaging under the supervision of H.T. and A.N.. T.O. generated H2B-GFP transgenic rice.

Competing Interests statement

The authors declare no competing financial interests.

Supplementary materials

Extended Data Figs. 1–4

418 **References**

419 1. Andrés, F. & Coupland, G. The genetic basis of flowering responses to seasonal cues.
420 *Nature Reviews Genetics* vol. 13 627–639 (2012).
421 2. Taoka, K.-I. *et al.* 14-3-3 proteins act as intracellular receptors for rice Hd3a florigen.
422 *Nature* **476**, (2011).
423 3. Collani, S., Neumann, M., Yant, L. & Schmid, M. FT Modulates Genome-Wide DNA-
424 Binding of the bZIP Transcription Factor FD. *Plant Physiol.* **180**, 367–380 (2019).
425 4. Li, C., Lin, H. & Dubcovsky, J. Factorial combinations of protein interactions generate a
426 multiplicity of florigen activation complexes in wheat and barley. *Plant J.* **84**, 70–82
427 (2015).
428 5. Chailakhyan, M. K. & Others. Hormonal theory of plant development. *Hormonal theory*
429 *of plant development.* (1937).
430 6. Zeevaart, J. A. D. Florigen coming of age after 70 years. *Plant Cell* **18**, 1783–1789
431 (2006).
432 7. Tamaki, S., Matsuo, S., Wong, H. L., Yokoi, S. & Shimamoto, K. Hd3a protein is a
433 mobile flowering signal in rice. *Science* **316**, 1033–1036 (2007).
434 8. Corbesier, L. *et al.* FT Protein Movement Contributes to Long-Distance Signaling in
435 Floral Induction of Arabidopsis. *Science* **316**, 1030–1033 (2007).
436 9. Kojima, S. *et al.* Hd3a, a Rice Ortholog of the Arabidopsis FT Gene, Promotes
437 Transition to Flowering Downstream of Hd1 under Short-Day Conditions. *Plant Cell*
438 *Physiol.* **43**, 1096–1105 (2002).
439 10. Tamaki, S. *et al.* FT-like proteins induce transposon silencing in the shoot apex during
440 floral induction in rice. *Proc. Natl. Acad. Sci. U. S. A.* **112**, E901–E910 (2015).
441 11. Abe, M. *et al.* FD, a bZIP protein mediating signals from the floral pathway integrator
442 FT at the shoot apex. *Science* **309**, 1052–1056 (2005).

443 12. Wigge, P. A. *et al.* Integration of spatial and temporal information during floral
444 induction in Arabidopsis. *Science* **309**, 1056–1059 (2005).
445 13. Hell, S. W. & Wichmann, J. Breaking the diffraction resolution limit by stimulated
446 emission: stimulated-emission-depletion fluorescence microscopy. *Opt. Lett.* **19**, 780–
447 782 (1994).
448 14. Klar, T. A., Jakobs, S., Dyba, M., Egner, A. & Hell, S. W. Fluorescence microscopy
449 with diffraction resolution barrier broken by stimulated emission. *Proc. Natl. Acad. Sci.*
450 *U. S. A.* **97**, 8206–8210 (2000).
451 15. Kobayashi, Y., Kaya, H., Goto, K., Iwabuchi, M. & Araki, T. A pair of related genes
452 with antagonistic roles in mediating flowering signals. *Science* **286**, 1960–1962 (1999).
453 16. Kardailsky, I. *et al.* Activation tagging of the floral inducer FT. *Science* **286**, 1962–1965
454 (1999).
455 17. Guivarc'H, A., Spena, A., Noin, M., Besnard, C. & Chriqui, D. The pleiotropic effects
456 induced by therolC gene in transgenic plants are caused by expression restricted to
457 protophloem and companion cells. *Transgenic Res.* **5**, 3–11 (1996).
458 18. Searle, I. *et al.* The transcription factor FLC confers a flowering response to
459 vernalization by repressing meristem competence and systemic signaling in Arabidopsis.
460 *Genes Dev.* **20**, 898–912 (2006).
461 19. Abiko, M., Maeda, H., Tamura, K., Hara-Nishimura, I. & Okamoto, T. Gene expression
462 profiles in rice gametes and zygotes: identification of gamete-enriched genes and up- or
463 down-regulated genes in zygotes after fertilization. *J. Exp. Bot.* **64**, 1927–1940 (2013).
464 20. Kurokawa, K., Ishii, M., Suda, Y., Ichihara, A. & Nakano, A. Chapter 14 - Live Cell
465 Visualization of Golgi Membrane Dynamics by Super-resolution Confocal Live Imaging
466 Microscopy. in *Methods in Cell Biology* (eds. Perez, F. & Stephens, D. J.) vol. 118 235–
467 242 (Academic Press, 2013).

468 21. Kurokawa, K. *et al.* Visualization of secretory cargo transport within the Golgi
469 apparatus. *J. Cell Biol.* **218**, 1602–1618 (2019).
470 22. Emenecker, R. J., Holehouse, A. S. & Strader, L. C. Emerging Roles for Phase
471 Separation in Plants. *Dev. Cell* **55**, 69–83 (2020).
472 23. Kim, J., Lee, H., Lee, H. G. & Seo, P. J. Get closer and make hotspots: liquid-liquid
473 phase separation in plants. *EMBO Rep.* **22**, e51656 (2021).
474 24. MacAlister, C. A. *et al.* Synchronization of the flowering transition by the tomato
475 TERMINATING FLOWER gene. *Nat. Genet.* **44**, 1393–1398 (2012).
476 25. Jung, J.-H. *et al.* A prion-like domain in ELF3 functions as a thermosensor in
477 Arabidopsis. *Nature* **585**, 256–260 (2020).
478 26. Fang, X. *et al.* Arabidopsis FLL2 promotes liquid-liquid phase separation of
479 polyadenylation complexes. *Nature* **569**, 265–269 (2019).
480 27. Huang, S., Zhu, S., Kumar, P. & MacMicking, J. D. A phase-separated nuclear GBPL
481 circuit controls immunity in plants. *Nature* **594**, 424–429 (2021).
482 28. Taoka, K.-I. *et al.* Novel assays to monitor gene expression and protein-protein
483 interactions in rice using the bioluminescent protein, NanoLuc. *Plant Biotechnol.* **38**,
484 89–99 (2021).
485 29. Cerise, M. *et al.* OsFD4 promotes the rice floral transition via florigen activation
486 complex formation in the shoot apical meristem. *New Phytol.* **229**, 429–443 (2021).
487 30. Serre, L., Vallée, B., Bureaud, N., Schoentgen, F. & Zelwer, C. Crystal structure of the
488 phosphatidylethanolamine-binding protein from bovine brain: a novel structural class of
489 phospholipid-binding proteins. *Structure* **6**, 1255–1265 (1998).
490 31. Banfield, M. J., Barker, J. J., Perry, A. C. & Brady, R. L. Function from structure? The
491 crystal structure of human phosphatidylethanolamine-binding protein suggests a role in
492 membrane signal transduction. *Structure* **6**, 1245–1254 (1998).

493 32. Hanzawa, Y., Money, T. & Bradley, D. A single amino acid converts a repressor to an
494 activator of flowering. *Proc. Natl. Acad. Sci. U. S. A.* **102**, 7748–7753 (2005).
495 33. Koornneef, M., Hanhart, C. J. & van der Veen, J. H. A genetic and physiological
496 analysis of late flowering mutants in Arabidopsis thaliana. *Mol. Gen. Genet.* **229**, 57–66
497 (1991).
498 34. Ahn, J. H. *et al.* A divergent external loop confers antagonistic activity on floral
499 regulators FT and TFL1. *EMBO J.* **25**, 605–614 (2006).
500 35. Ho, W. W. H. & Weigel, D. Structural Features Determining Flower-Promoting Activity
501 of Arabidopsis FLOWERING LOCUS T. *Plant Cell* **26**, 552–564 (2014).
502 36. Nakagawa, T. *et al.* Development of series of gateway binary vectors, pGWBs, for
503 realizing efficient construction of fusion genes for plant transformation. *J. Biosci.*
504 *Bioeng.* **104**, 34–41 (2007).
505 37. Hellens, R. P., Edwards, E. A., Leyland, N. R., Bean, S. & Mullineaux, P. M. pGreen: a
506 versatile and flexible binary Ti vector for Agrobacterium-mediated plant transformation.
507 *Plant Mol. Biol.* **42**, 819–832 (2000).
508 38. Nakamura, S. *et al.* Gateway binary vectors with the bialaphos resistance gene, bar, as a
509 selection marker for plant transformation. *Biosci. Biotechnol. Biochem.* **74**, 1315–1319
510 (2010).
511 39. Taoka, K.-I., Ham, B.-K., Xoconostle-Cázares, B., Rojas, M. R. & Lucas, W. J.
512 Reciprocal phosphorylation and glycosylation recognition motifs control NCAPP1
513 interaction with pumpkin phloem proteins and their cell-to-cell movement. *Plant Cell*
514 **19**, 1866–1884 (2007).
515 40. Takeda, A. *et al.* Identification of a novel RNA silencing suppressor, NSs protein of
516 Tomato spotted wilt virus. *FEBS Lett.* **532**, 75–79 (2002).
517 41. Higo, A. *et al.* DNA methylation is reconfigured at the onset of reproduction in rice

518 shoot apical meristem. *Nat. Commun.* **11**, 4079 (2020).

519 42. Hayashi, K. & Kojima, C. pCold-GST vector: a novel cold-shock vector containing GST
520 tag for soluble protein production. *Protein Expr. Purif.* **62**, 120–127 (2008).

521 43. Purwestri, Y. A., Ogaki, Y., Tamaki, S., Tsuji, H. & Shimamoto, K. The 14-3-3 protein
522 GF14c acts as a negative regulator of flowering in rice by interacting with the florigen
523 Hd3a. *Plant Cell Physiol.* **50**, (2009).

524 44. Jawerth, L. *et al.* Protein condensates as aging Maxwell fluids. *Science* **370**, 1317–1323
525 (2020).

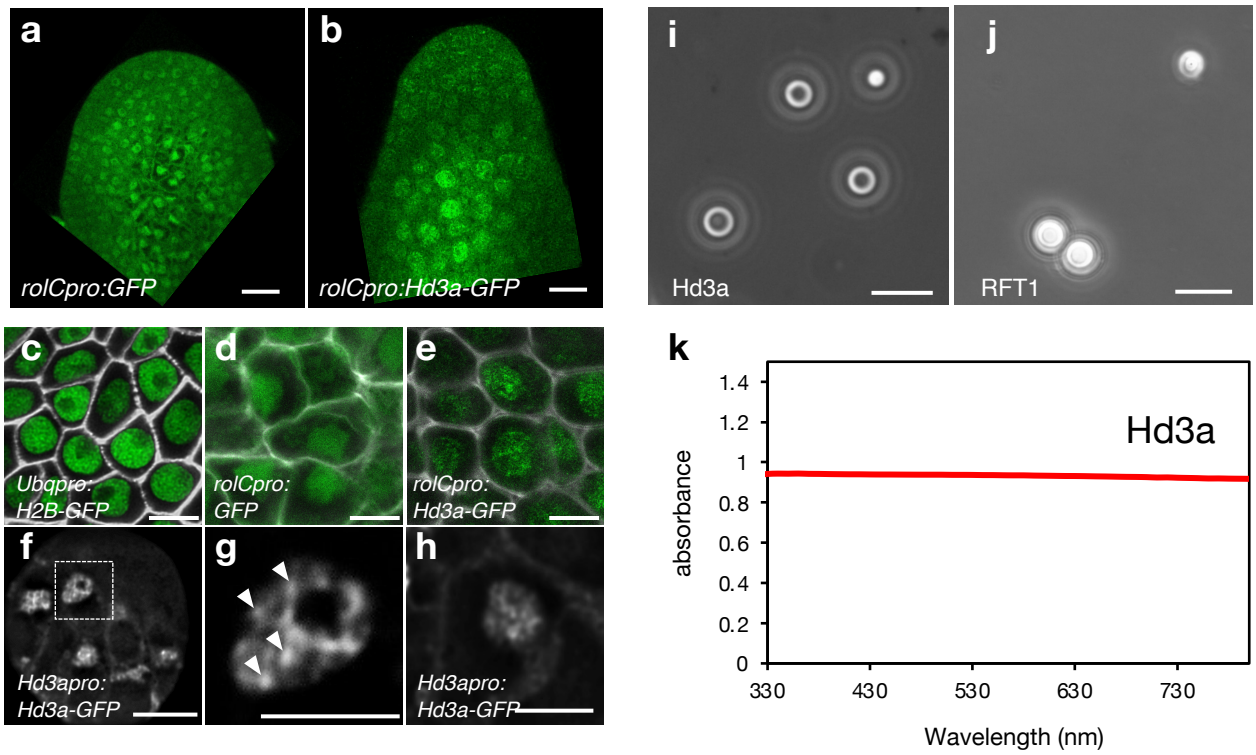
a
rolCpro:GFP
b
rolCpro:Hd3a-GFP
i
Hd3a
j
RFT1
c
Ubqpro:
H2B-GFP
d
rolCpro:
GFP
e
rolCpro:
Hd3a-GFP
f
Hd3apro:
Hd3a-GFP
g
h
Hd3apro:
Hd3a-GFP
k
Hd3a
absorbance
1.4
1.2
1
0.8
0.6
0.4
0.2
0
330
430
530
630
730
Wavelength (nm)

Fig. 1

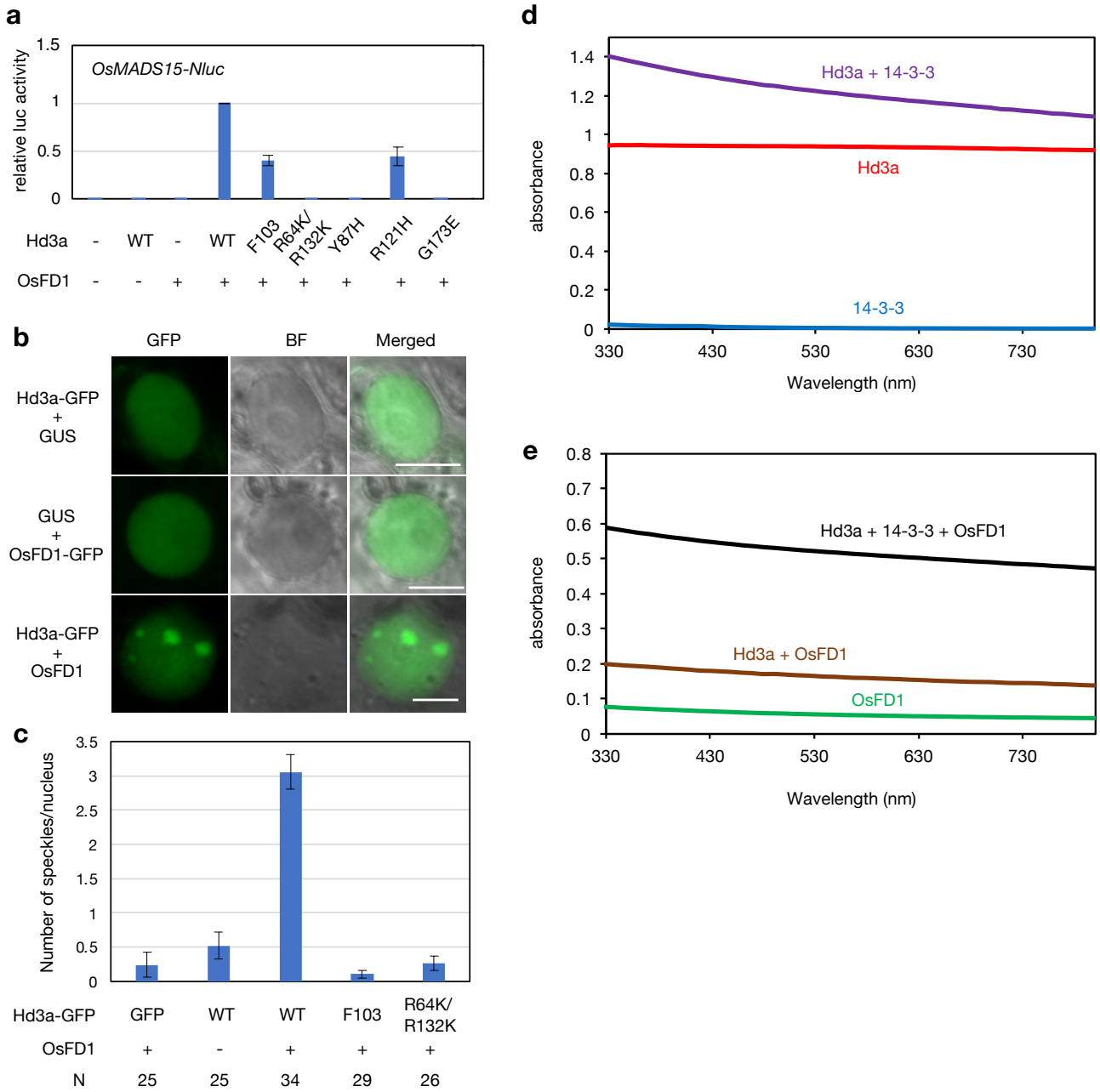
a
OsMADS15-Nluc
relative luc activity
1.5
1
0.5
0
Hd3a - WT - WT F103 R64K/ R132K Y87H R121H G173E
OsFD1 - - + + + + + + +
b
GFP
BF
Merged
Hd3a-GFP + GUS
GUS + OsFD1-GFP
Hd3a-GFP + OsFD1
c
Number of speckles/nucleus
3.5
3
2.5
2
1.5
1
0.5
0
Hd3a-GFP GFP WT WT F103 R64K/ R132K
OsFD1 + - + + +
N 25 25 34 29 26
d
absorbance
Hd3a + 14-3-3
Hd3a
14-3-3
1.4
1.2
1
0.8
0.6
0.4
0.2
0
330 430 530 630 730
Wavelength (nm)
e
absorbance
Hd3a + 14-3-3 + OsFD1
Hd3a + OsFD1
OsFD1
0.8
0.7
0.6
0.5
0.4
0.3
0.2
0.1
0
330 430 530 630 730
Wavelength (nm)

Fig. 2

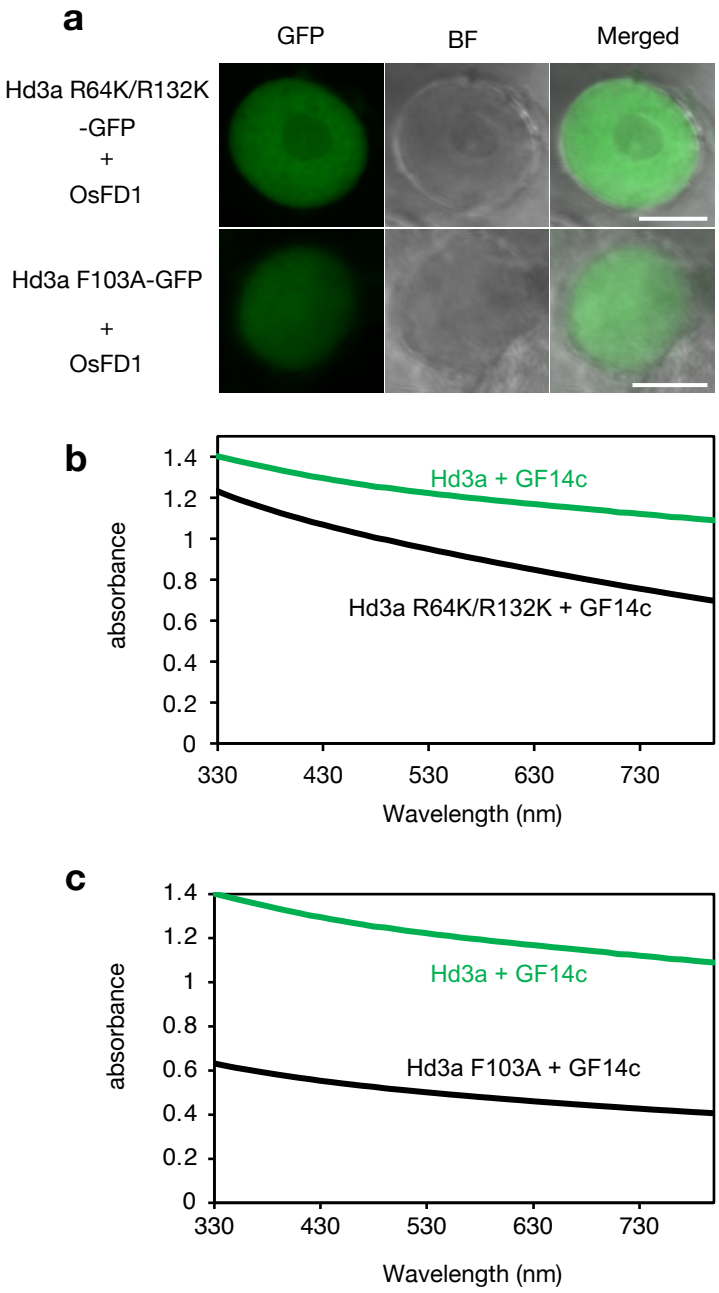
a
GFP
BF
Merged
Hd3a R64K/R132K
-GFP
+
OsFD1
Hd3a F103A-GFP
+
OsFD1
b
absorbance
1.4
1.2
1
0.8
0.6
0.4
0.2
0
330
430
530
630
730
Wavelength (nm)
Hd3a + GF14c
Hd3a R64K/R132K + GF14c
c
absorbance
1.4
1.2
1
0.8
0.6
0.4
0.2
0
330
430
530
630
730
Wavelength (nm)
Hd3a + GF14c
Hd3a F103A + GF14c

Fig. 3

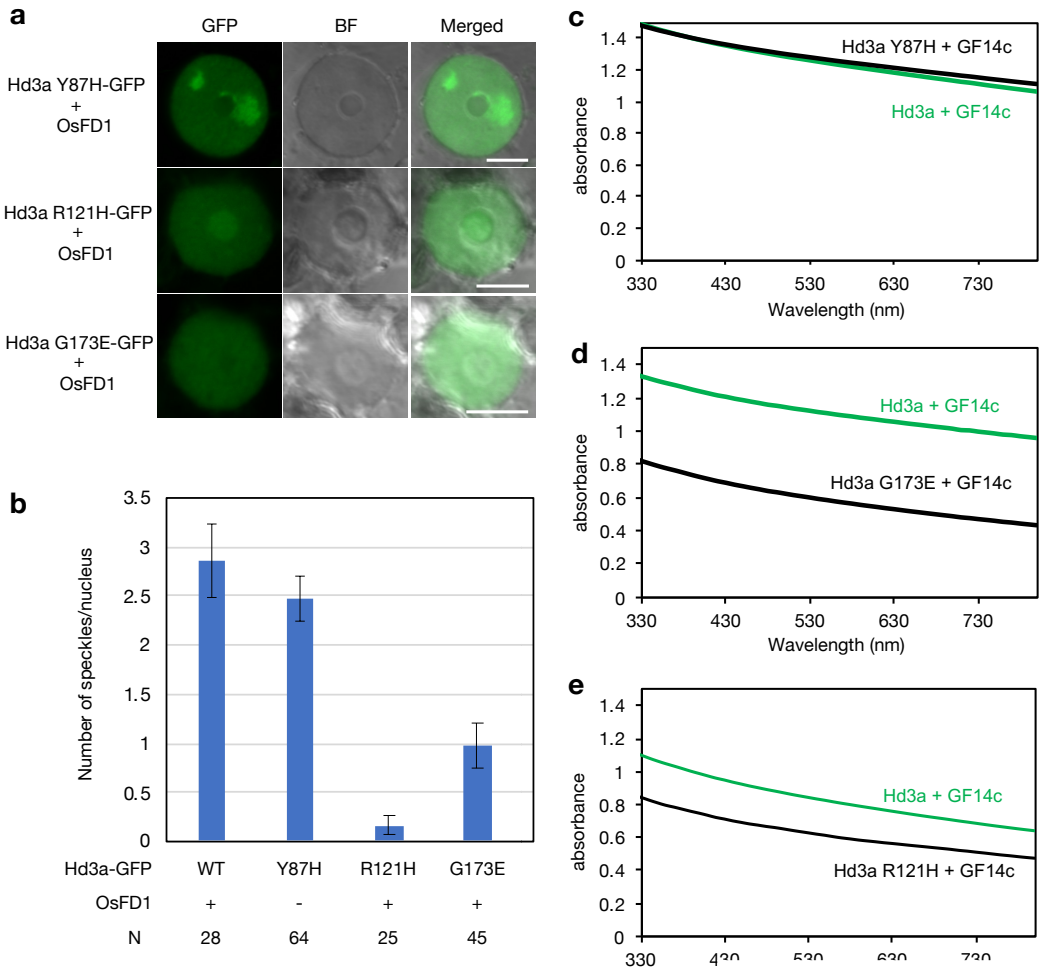
a
GFP
BF
Merged
Hd3a Y87H-GFP + OsFD1
Hd3a R121H-GFP + OsFD1
Hd3a G173E-GFP + OsFD1
b
Number of speckles/nucleus
Hd3a-GFP
WT
Y87H
R121H
G173E
OsFD1
N
28
64
25
45
c
Hd3a Y87H + GF14c
Hd3a + GF14c
absorbance
Wavelength (nm)
d
Hd3a + GF14c
Hd3a G173E + GF14c
e
Hd3a + GF14c
Hd3a R121H + GF14c

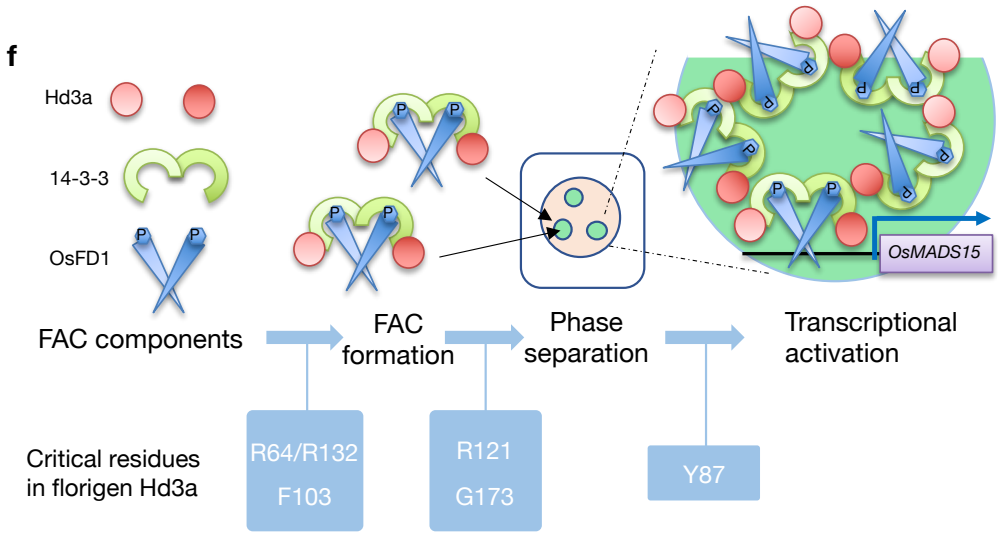
f
Hd3a
14-3-3
OsFD1
FAC components
FAC formation
Phase separation
Transcriptional activation
OsMADS15
Critical residues in florigen Hd3a
R64/R132
F103
R121
G173
Y87

Fig. 4

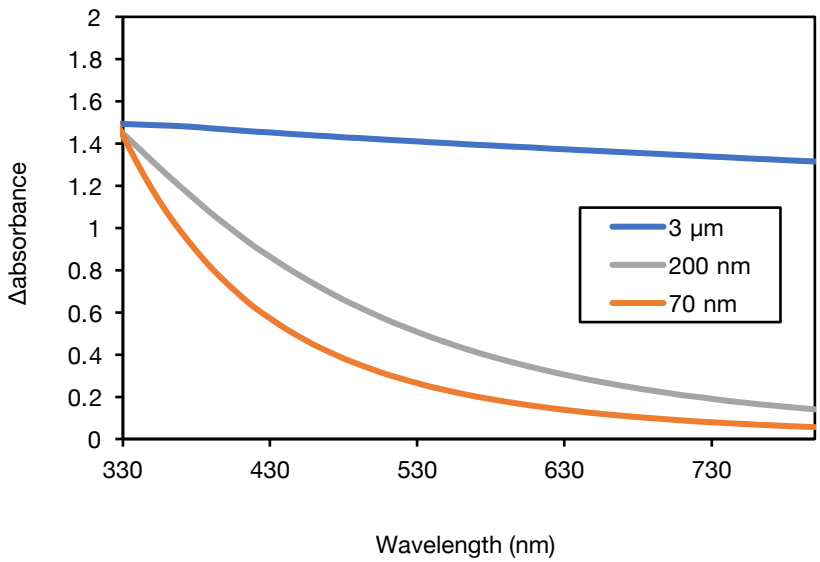

Extended Data Fig. 1

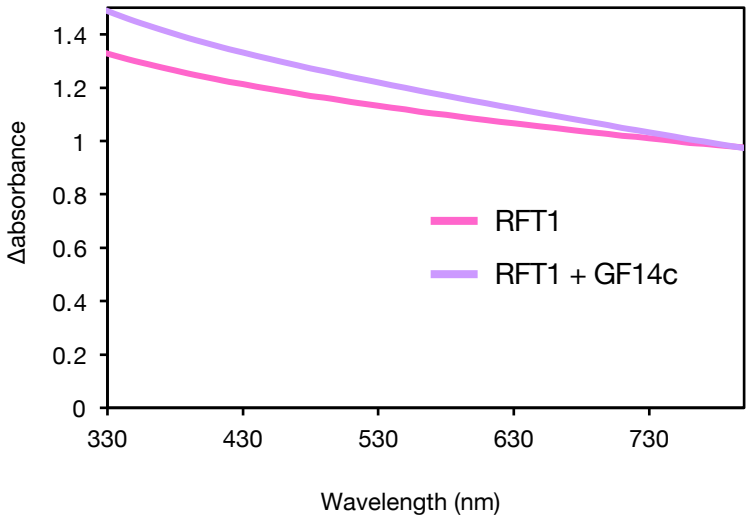

Extended Data Fig. 2

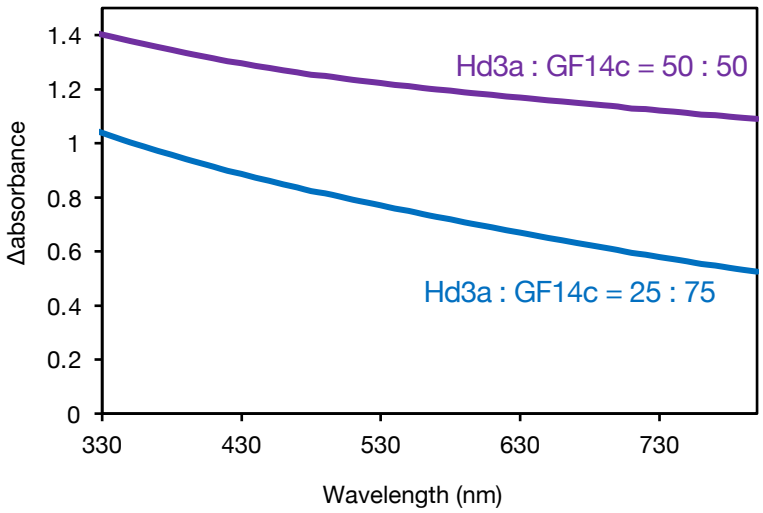

Extended Data Fig. 3

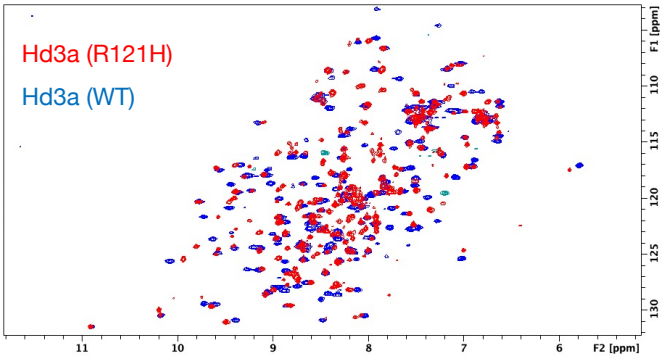

Extended Data Fig. 4